Macromolecular Rapid Communications
www.mrc-journal.de

Spatiotemporal Control Over Base-Catalyzed Hydrogelation Using a Bilayer System

*Paolo Ravarino, Santanu Panja, and Dave J. Adams**

Controlling the formation and directional growth of hydrogels is a challenge. In this paper, a new methodology to program the gel formation both over space and time is proposed, using the diffusion and subsequent hydrolysis of 1,1′-carbonyldiimidazole from an immiscible organic solution to the aqueous gel media.

1. Introduction

Low-molecular-weight gels are interesting soft materials behaving both as solid and liquid. The solid-like behavior arises from the presence of fibers inside that form the matrix and entrap the solvent through surface tension resulting in an increase in viscosity of the materials.[1] The fibers are formed through weak noncovalent interactions between the molecules.[2] The existing noncovalent interactions can be easily perturbed by applying an external stimulus[3] which makes them suitable for many applications, for example in drug delivery[4] and optoelectronics.[5] Due to the high tunability of these systems, such materials are often called "smart" or "intelligent" materials.

Typically, gels are prepared by applying a trigger like temperature, UV-light, pH, or additional ions that substantially reduces the solubility of the organic molecules in the solution. For instance, molecules possessing a basic group such as amines are usually soluble under acidic conditions where these moieties are protonated and form polar ammonium salts. When the pH increases, the ammonium groups undergo deprotonation, resulting in a decrease in polarity and aqueous solubility, enabling the formation of fibrous structures.[6]

P. Ravarino
Dipartimento di Chimica Giacomo Ciamician
Alma Mater Studiorum
Università di Bologna
Via Selmi, 2, Bologna 40126, Italy
S. Panja, D. J. Adams
School of Chemistry
University of Glasgow
Glasgow G12 8QQ, UK
E-mail: dave.adams@glasgow.ac.uk

The ORCID identification number(s) for the author(s) of this article can be found under https://doi.org/10.1002/marc.202200606

DOI: 10.1002/marc.202200606

However, there are some limitations in the preparation of these materials. Low-molecular-weight gels are quite weak, breaking at low strain, and controlling their gelation can be challenging. Recently, efforts have been made to pattern such gels. For example, a photo-responsive gelator can undergo gel-to-sol or sol-to-gel transition by irradiation with light. It is possible to photo-pattern these gels either by applying a mask or by using a light source as a confocal laser.[7] However, photoresponsive gelators demand a photo-sensitive unit on the skeleton for activation. Moreover, use of photoinitiators or the byproducts generated upon photoirradiation not only influences the material properties but also limits the application of these gels, particularly in biology.[8]

Controlling the diffusion is another interesting way to achieve spatial control. In this case, two or more species are initially spatially separated. Their diffusion is accompanied by a reaction that generates (or triggers) the gelator and consequently, local structures are formed.[9] This kind of system usually works heterogeneously. For example, the diffusion of ammonia vapor into the gelator medium can be used to prepare gradient gels.[10] Bilayer systems are often used for controlling the diffusion and the formation of gels, as when the layers are two immiscible solvents or when they are physically separated.[11] For instance, Nishida et al. showed in situ synthesis of a dynamic covalent hydrogelator by exploiting diffusion of an aldehyde from an organic layer into the aqueous layer containing an amine yielding a gel.[12] These systems are elegant, as it is possible to obtain a gradient of diffusion and therefore the formation of gradient or multilayer gels. The use of compartmentalized enzymes is an intriguing recent method for efficiently achieving spatiotemporal control.[13] For example, Mai et al. studied the production of a hydrogel coating by exploiting the reaction-diffusion method. In a solution containing the gelator and urea in an acidic aqueous phase, particles with the enzyme urease immobilized on them were dispersed. The production of ammonia on the particles caused an increase in the pH localized on the surface of the particles, causing the formation of a hydrogel in that region and therefore a gel coating.[9b]

Here, we describe the controlled formation of a hydrogel from the Fmoc-functionalized gelator **1** (**Figure 1**a) over space and time involving a water/organic bilayer system. Typically, gelators possessing a hydrophilic head and a hydrophobic tail group often behave like a surfactant above a critical concentration.[14] The surfactant-like behavior of gelators in an organic/water bilayer system has been extensively studied by the Ulijn group. They exploited the interfacial activity of surfactant-like hydrogelators to trigger nanofiber formation at the chloroform/water interface and thereby stabilize the oil-in-water emulsions involving their

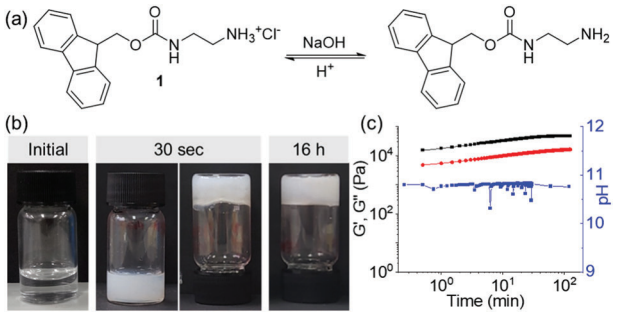

Figure 1. a) pH-responsive changes in the chemical structure of **1**. b) Photographs of the phase changes of the aqueous solution of **1** (left) with time on addition of NaOH. c) Variation of G′ (black), G″ (red), and pH (blue) with time for **1** in presence of NaOH. For (b,c) the concentration of **1** is 10 mg mL^{-1}, concentration of NaOH is 1 equimolar with respect to **1**.

physical interactions with the solvents.[15] However, here we employed the water/organic bilayer system with a different goal to achieve control over the pH of the aqueous layer by performing a chemical reaction at the organic/water interface. When a hydrolyzing reagent is incorporated into the organic layer, hydrolysis of the compound at the water/organic interface drives the pH change in the aqueous layer and triggers the formation and growth of the gel from the interface to the bottom of the aqueous layer. Variation of the concentration of the hydrolyzing reagent in the organic layer further enables control of the final properties of the materials.

2. Results and Discussion

Compound **1** undergoes deprotonation on increasing pH and forms a self-supported gel in H_2O very quickly at a concentration of 10 mg mL^{-1} (Figure 1b).[6c] In presence of equimolar amounts of NaOH, the pH of the gel was measured to be 9.8. Time sweep rheology shows that the initial value of storage modulus (G′) was significantly greater than the loss modulus (G″), suggesting a gel was being formed even before the measurement could begin (Figure 1c). To achieve spatiotemporal control over the gelation of **1**, we used 1,1′-carbonyldiimidazole (CDI) as a chemical reagent to trigger the pH change. CDI reacts with water and produces carbon dioxide and imidazole resulting in an increase in pH (**Figure 2**a).[16] However, the hydrolysis of CDI is vigorous which makes the process uncontrollable.[16] Therefore, instead of using CDI directly to trigger the pH change of the solution of **1** (in water), we devised a water/organic bilayer system and incorporated the CDI into the organic layer. We used tert-butyl methyl ether (TBME) as the organic solvent. This allows for slow diffusion of CDI from the immiscible TBME layer into the aqueous layer followed by hydrolysis and gradual pH increase of the aqueous layer. Visually, the gel starts forming from the water/organic interface and propagates to the bottom over time (Figure 2b). Figure 2c reveals a sigmoidal curve for the pH-time profile of the aqueous layer with a gradual increase of pH from ≈4 to ≈7.7. In designing the bilayer system, organic solvents such as DMF, THF, DMSO, and 1,4-dioxane were discarded because of their high miscibility with water. In contrast, water-immiscible organic solvents such as toluene, chloroform, and ethyl acetate were avoided after finding the amine (after freeze-drying the NaOH triggered gel) soluble in these solvents. We optimized using TBME as the organic solvent because of poor solubility of the amine in TBME. Diethyl ether was also avoided in the study because of its higher volatility than TBME. The gel obtained using the bilayer approach was found to be stable over several days in contact with TBME.

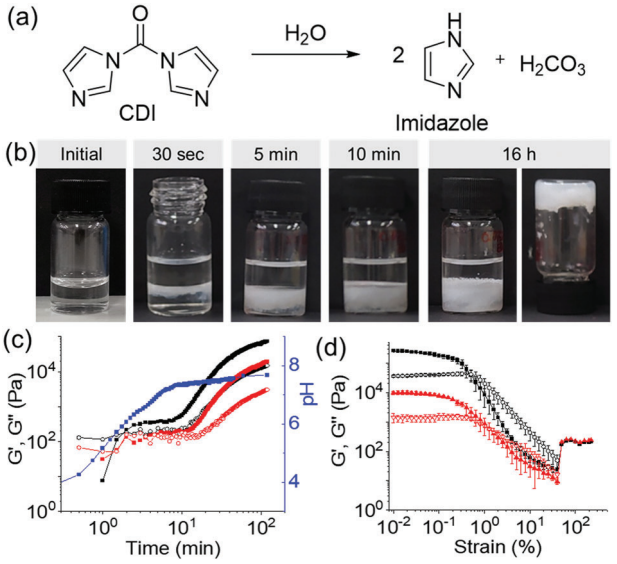

Figure 2. a) Reaction showing the hydrolysis of CDI (1,1′-carbonyldiimidazole) producing imidazole. b) Photographs showing the phase changes of the aqueous solution of **1** over time in contact with CDI solution in TBME. c) Variation of pH (blue), G′ (solid symbols), and G″ (open symbols) with time for **1** with CDI involving the bilayer system when the shaft is positioned at 6 (black) and 4 mm (red) from the bottom. d) Strain sweeps of the hydrogels of **1** obtained with 1 equiv. of NaOH (black) and in contact with the solution of CDI in TBME (red). Solid symbols represent G′, hollow symbols represent G″. For (b–d) the initial concentration of CDI is 0.075 M and the volume of TBME is 2 mL. In all cases, the concentration of **1** is 10 mg mL^{-1} and the volume of the aqueous layer is 2 mL.

A parallel plate geometry was used for rheological time sweeps to probe the gelation of **1** at different levels of the aqueous layer with the pH increase (Figure S1, Supporting Information). First, the shaft of the parallel plate was positioned at a height close to the water/organic interface (at 6 mm from the bottom) and the variations of rheological moduli (G′, G″) over time were recorded (Figure 2c). Initially, the values of storage modulus (G′) were very close to the corresponding loss modulus (G″) indicating that the self-assembled structures were weak at the initial stages. Typically, the gelation begins after ≈8 min which was evident from the sudden increase of both G′ and G″ values. Over time, both G′ and G″ increased significantly suggesting that the self-assembled network became stronger over time. Unlike using NaOH, the bilayer approach allowed the gel to grow from the top to bottom of the aqueous layer (Figure 2b). To understand the spatial control over gel formation, a rheological time sweep was conducted under similar conditions but by placing the shaft at a different height (4 mm from the bottom of the vial). On moving down from the water/organic interface, the increase of rheological moduli and complex viscosity was delayed considerably compared to measurements at the top. These results confirm the formation and propagation of the gel from the top to the bottom, agreeing with

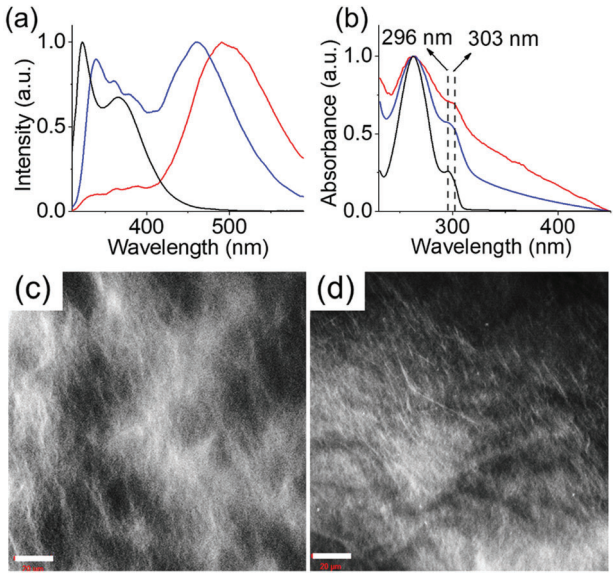

Figure 3. Normalized a) emission and b) UV–vis spectra of the solution of **1** (black), and the gels obtained from **1** with 1 equiv. of NaOH (red) and with CDI involving the bilayer system (blue). c,d) Confocal microscopy images (scale bar is 20 μm) of the gels obtained from **1** c) with 1 equiv. of NaOH and d) with CDI involving the bilayer system. For (d), the sample was taken from the bottom of the gel. For (a,b,d), the concentration of CDI is 0.075 M and the volume of TBME is 2 mL. In all cases, the concentration of the **1** is 10 mg mL^{-1} and the volume of the aqueous layer is 2 mL.

the visual observations. Slippage during measurement could be a concern. However, here we have no sign of a sudden drop in the rheological moduli so we do not believe slip is occurring in these measurements. Typically, CDI is used in organic synthesis to obtain amide, urea, and carbamate derivatives from amines.[17] However, in our case, HRMS analysis revealed the mass value for the amine form of **1** in the gel state and no mass for the homourea of **1** was found (Figure S2, Supporting Information). Proton NMR experiments confirm the stability of the corresponding amine of **1** in the gel state without any deprotection of the Fmoc group (Figure S3, Supporting Information). Moreover, the signatures of imidazole protons coexist with compound **1** implying the hydrolysis of CDI to imidazole (Figure S3, Supporting Information). Whilst we cannot rule out a tiny amount of TBME in the gel phase, its low solubility in water makes this unlikely.

The final pH of the CDI-triggered gel (using the bilayer approach) was recorded to be 7.7, significantly lower than the NaOH treated gel (pH 9.8). The apparent pK_a of **1** is above 8.0. [6c] This indicates that the gel was formed at a pH lower than the pK_a of the gelator possibly due to its high concentration or because **1** tends to form aggregates with the imidazolium ions. The lower pH of the CDI-triggered gel resulted in a reduction in the stiffness (G′) of the gel compared to that obtained using NaOH (Figure 2d; Figure S4, Supporting Information). A decrease in the final pH typically reduces the extent of deprotonation of **1** and subsequently lowers the concentration of the corresponding amine responsible for gelation. To understand this, fluorescence studies were conducted with the gels (**Figure 3**a; Figure S5, Supporting Information). The solution of **1** exhibited a strong emission at 322 nm and a relatively less intensified peak at 366 nm corresponding to the monomer and excimer emission of the Fmoc-group, respectively.[18] The excimer peak at 366 nm appeared due to the parallel overlapping of the fluorenyl groups.[14c] In the CDI-triggered gel at pH 7.7, the monomer emission of **1** red-shifted to 338 nm along with a simultaneous emergence of a new peak at 460 nm derived from the antiparallel overlapping of the fluorenyl groups. [18] Interestingly, the monomer emission of **1** was almost fully quenched in the NaOH triggered gel at pH 9.8 and the excimer emission (antiparallel fashion) was predominant at 490 nm. These results indicate that the degree of deprotonation of **1** is higher at pH 9.8, enabling the amine to contribute more to self-assembly involving aromatic stacking. In contrast, the existence of the nongelling ammonium form of **1** in the CDI-triggered gel corroborates the lower stiffness of the material. To further understand this, UV–vis and FTIR studies were performed (Figure 3b; Figure S6, Supporting Information). The absorbance of the solution of **1** at 296 nm was red shifted in both the gels (Figure 3b). However, the red shift is more prominent for the gel formed using NaOH. By FTIR spectroscopy, the carbamate carbonyl stretching of **1** at 1714 cm^{-1} moved to the lower values of 1688 and 1683 cm^{-1} in the gel with CDI and NaOH, respectively (Figure S6, Supporting Information). These results agree with the higher extent of deprotonation of **1** in the presence of NaOH leading to the formation of a stronger hydrogel network involving the amine. There was also a difference in the microstructures of the gels noticed under the confocal microscope. Note that the drying of gels often results in changes in the self-assembled structures and so confocal microscopy was used for imaging the gels under wet conditions (without drying or freezing).[19] Although in both cases spherulitic domains of fibers are formed, the spherulites are larger in size for the NaOH triggered gel (Figure 3c,d; Figure S7, Supporting Information). No significant change in the fibrous structure was noticed along the diffusion direction of imidazole, as such it is difficult to conclude if the fibers are aligned along the diffusion direction of the base.

To better understand the temporal aspect of gelation, similar experiments were carried out with the aqueous solution of **1** by manipulating either the concentration of CDI or the volume of the CDI solution added (**Figure 4**; Figure S8, Supporting Information). The rate of pH change for the aqueous layer was influenced considerably by the variation of the total amount of CDI present in the organic layer (Figure S9, Supporting Information). The pH versus time curve was no longer sigmoidal on increasing the volume of the CDI solution (0.075 M) from 2 mL (total amount of CDI is 0.150 mmol, Figure 2c) to 3 mL (total amount of CDI is 0.225 mmol, Figure 4a), and a rapid increase in pH with time was observed. In contrast, sigmoidal pH-time profiles with a significant delay in the lag phase (i.e., the time before the pH jump) were observed either on decreasing the concentration of CDI solution (2 mL of 0.050 M, total amount of CDI is 0.100 mmol, Figure 4b) or by increasing the volume of the CDI solution keeping the total amount of CDI unchanged (3 mL of 0.050 M, total amount of CDI is 0.150 mmol, Figure 4c). Noticeably, the rate of gelation depends upon the initial reaction conditions. Time sweep rheology shows that the time required for gelation follows similar trends as that of pH which was more prominent in the cases where the pH change was slow. As observed, the increase of G′ and G″ was delayed significantly with the decrease in the rate of pH change. However, the final pH of the gels was

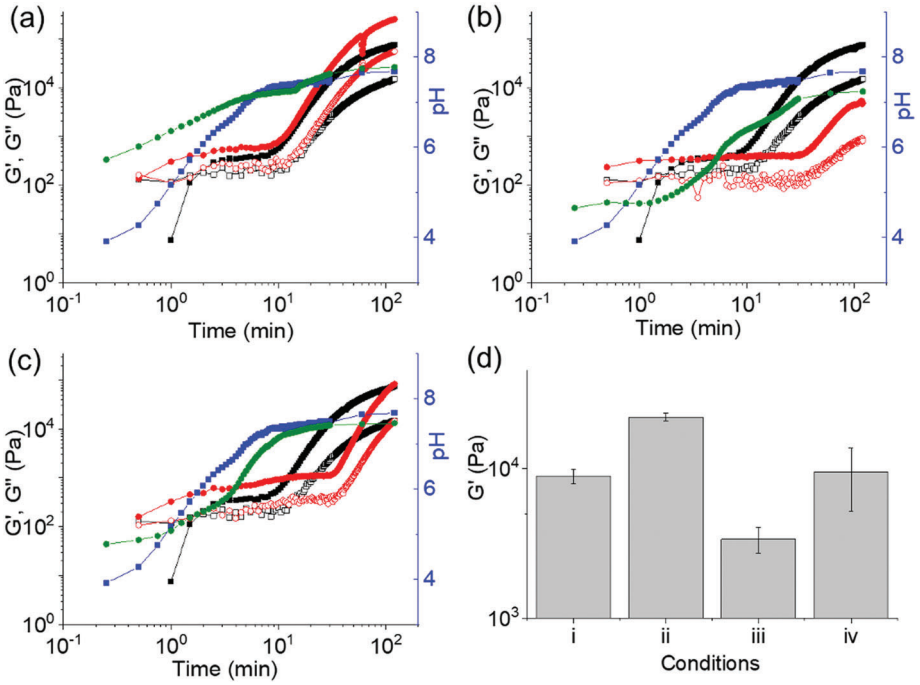

Figure 4. Spatiotemporal programming: a–c) Changes in rheological moduli (red data) on the variation of pH (green) with time for the hydrogel of **1** with CDI involving bilayer systems under different conditions: a) [CDI] = 0.075 M, volume of CDI solution = 3 mL; b) [CDI] = 0.050 M, volume of CDI solution = 2 mL; c) [CDI] = 0.050 M, volume of CDI solution = 3 mL. For (a–c), the blue and black data represent the variation of pH and rheological moduli, respectively, for **1** involving the bilayer system under conditions: [CDI] = 0.075 M, volume of CDI solution = 2 mL. The blue and black data are overlayed to compare the variations of pH and rheological moduli, respectively, on changing the reaction conditions. For black and red rata, the solid symbols represent G′, the open ones G″. For all the time sweeps, the shaft is positioned at 6 mm from the bottom. d) Bar graph comparing the stiffness (at $\gamma = 0.05\%$) of the gels obtained from **1** with CDI involving the bilayer system under different conditions: i) [CDI] = 0.075 M, volume of CDI solution = 2 mL; ii) [CDI] = 0.075 M, volume of CDI solution = 3 mL; iii) [CDI] = 0.050 M, volume of CDI solution = 2 mL; and iv) [CDI] = 0.050 M, volume of CDI solution = 3 mL. For (a–d) the concentration of **1** is 10 mg mL^{-1} and the volume of the aqueous layer is 2 mL.

not influenced by the rate of pH change. It rather depends on the total CDI content. The pH of the gels changes proportionally as with the increase or decrease of the total CDI amount (Table S1, Supporting Information). As a consequence, the stiffness of the final gels varies accordingly to the final pH (Figure 4d; Figure S10, Supporting Information). As such, we are able to not only program the hydrogel temporally but also control the final material properties of the gels simply by varying the initial reaction conditions and so by controlling the final pH.

Finally, to investigate if the bilayer approach is suitable in general to prepare base-triggered hydrogels, we applied the same methodology to compound **2** (**Figure 5**), sharing a similar structure. Like, **1**, the hydrogel formed by **2** appeared in a spatiotemporal manner. However, the pH-time profile and the time sweep rheology for system **2** showed significant differences compared to **1** with a decrease in the rate of pH change and a delay in the appearance of the gel, respectively. The hydrogel of **2** exhibited long fibers under confocal microscope. These results confirm that our bilayer approach using CDI can be applied in general to prepare base-triggered hydrogels.

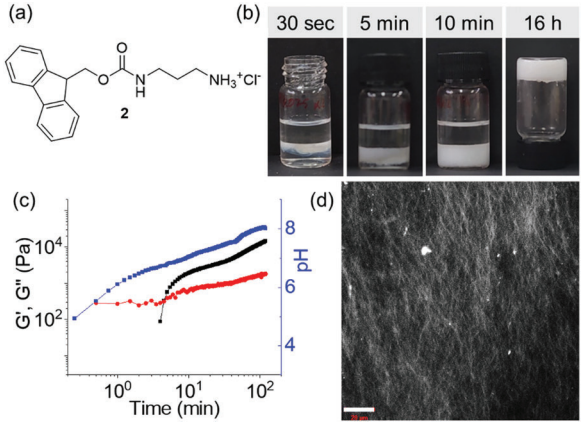

Figure 5. a) Chemical structure of the compound **2**. b) Photographs showing the phase changes of the aqueous solution of **2** over time in contact with CDI solution in TBME. c) variation of pH (blue), G′ (black), and G″ (red) over time for **2** in presence of CDI involving the bilayer system. d) Confocal microscopy image (scale bar is 20 μm) of the gel of **2** obtained from CDI involving the bilayer system. For (b–d) the concentration of **2** is 10 mg mL^{-1}, the volume of the aqueous layer is 2 mL, the concentration of CDI is 0.075 M, and the volume of TBME is 2 mL.

3. Conclusion

To summarize, we have devised a new reaction-diffusion methodology for programming the hydrogel formation over space and time using CDI and a bilayer system of two immiscible solvents. Tuning the reaction-diffusion is simple and the rate of gel formation can be controlled in many ways. Variation of the total CDI concentration in the organic phase modulates the rate of

gel formation in the aqueous layer, whilst the final properties of the gels are dependent on the total amount of CDI and not related to the gelation rate. A literature survey reveals a large number of gelators contain pH-responsive amine-groups. However, there are limited methodologies available for increasing the pH and thereby synthesizing base-triggered gels.[20] In this context, CDI-triggered control over the pH increase is new. We envisage that our method can be extended to other hydrogelators with an amine functionality and could be useful in more complex systems such as multicomponent materials. Spatiotemporal programming of gels is widely used to create micro and nano structured architectures in artificial life-like systems, [12,21] allowing access to materials with a gradient in properties which are potentially applicable in tissue engineering, cell culture, etc. [21b,22] We anticipate that our concept could be extended further to control diffusion gradients across gels for reaction-based systems, for example, reaction in localized sites followed by diffusion of the products across the gels controlled by the pH.

4. Experimental Section

Full experimental details, further rheology, time sweep data, and confocal microscopy. The Supporting Information is available free of charge on the Wiley website as a PDF document.

Supporting Information

Supporting Information is available from the Wiley Online Library or from the author.

Acknowledgements

P.R. thanks the University of Bologna for Marco Polo funding. S.P. thanks the University of Glasgow for funding.

Conflict of interest

The authors declare no conflict of interest.

Data Availability Statement

The data that support the findings of this study are available in the supplementary material of this article.

Keywords

bilayer system, carbonyldiimidazole, pH-responsiveness, reaction-diffusion, rheology, self-assembly

Received: July 8, 2022
Revised: August 11, 2022
Published online: September 6, 2022

[1] a) P. Terech, R. G. Weiss, *Chem. Rev.* **1997**, *97*, 3133; b) L. A. Estroff, A. D. Hamilton, *Chem. Rev.* **2004**, *104*, 1201.
[2] a) E. R. Draper, D. J. Adams, *Chem. Soc. Rev.* **2018**, *47*, 3395; b) N. M. Sangeetha, U. Maitra, *Chem. Soc. Rev.* **2005**, *34*, 821.
[3] J. Zhang, Y. Hu, Y. Li, in *Gel Chemistry: Interactions, Structures and Properties* (Eds: J. Zhang, Y. Hu, Y. Li), Springer Singapore, Singapore **2018**, p. 9.
[4] a) M. Halder, Y. Bhatia, Y. Singh, *Biomater. Sci.* **2022**, *10*, 2248; b) M. Rodrigues, A. C. Calpena, D. B. Amabilino, M. L. Garduño-Ramírez, L. Pérez-García, *J. Mater. Chem. B* **2014**, *2*, 5419.
[5] a) A. Panja, P. Bairi, D. Halder, S. Das, A. K. Nandi, *J. Colloid Interface Sci.* **2020**, *579*, 531; b) H. Zhang, J. Cheng, Q. Zhou, Q. Zhang, G. Zou, *Soft Matter* **2020**, *16*, 5203.
[6] a) P. Lundberg, N. A. Lynd, Y. Zhang, X. Zeng, D. V. Krogstad, T. Paffen, M. Malkoch, A. M. Nyström, C. J. Hawker, *Soft Matter* **2013**, *9*, 82; b) A. Jain, S. Dhiman, A. Dhayani, P. K. Vemula, S. J. George, *Nat. Commun.* **2019**, *10*, 450; c) S. Panja, D. J. Adams, *Chem. Commun.* **2019**, *55*, 47.
[7] a) D. J. Cornwell, O. J. Daubney, D. K. Smith, *J. Am. Chem. Soc.* **2015**, *137*, 15486; b) J. Eastoe, M. Sánchez-Dominguez, P. Wyatt, R. K. Heenan, *Chem. Commun.* **2004**, 2608; c) A. Legrand, L.-H. Liu, P. Royla, T. Aoyama, G. A. Craig, A. Carné-Sánchez, K. Urayama, J. J. Weigand, C.-H. Lin, S. Furukawa, *J. Am. Chem. Soc.* **2021**, *143*, 3562.
[8] L. Thomson, R. Schweins, E. R. Draper, D. J. Adams, *Macromol. Rapid Commun.* **2020**, *41*, 2000093.
[9] a) M. Lovrak, W. E. J. Hendriksen, C. Maity, S. Mytnyk, V. Van Steijn, R. Eelkema, J. H. Van Esch, *Nat. Commun.* **2017**, *8*, 15317; b) A. Q. Mai, T. Bánsági, A. F. Taylor, J. A. Pojman, *Commun. Chem.* **2021**, *4*, 101.
[10] a) A. Mata, L. Hsu, R. Capito, C. Aparicio, K. Henrikson, S. I. Stupp, *Soft Matter* **2009**, *5*, 1228; b) P. Liu, C. Mai, K. Zhang, *Front. Chem. Sci. Eng.* **2018**, *12*, 383.
[11] a) V. Lakshminarayanan, L. Poltorak, D. Bosma, E. J. R. Sudhölter, J. H. van Esch, E. Mendes, *Chem. Commun.* **2019**, *55*, 9092; b) H. S. Cooke, L. Schlichter, C. C. Piras, D. K. Smith, *Chem. Sci.* **2021**, *12*, 12156.
[12] Y. Nishida, A. Tanaka, S. Yamamoto, Y. Tominaga, N. Kunikata, M. Mizuhata, T. Maruyama, *Angew. Chem., Int. Ed.* **2017**, *56*, 9410.
[13] X. Fan, A. Walther, *Angew. Chem., Int. Ed.* **2021**, *60*, 3619.
[14] a) S. Fleming, S. Debnath, P. W. J. M. Frederix, N. T. Hunt, R. V. Ulijn, *Biomacromolecules* **2014**, *15*, 1171; b) T. Li, M. Kalloudis, A. Z. Cardoso, D. J. Adams, P. S. Clegg, *Langmuir* **2014**, *30*, 13854; c) S. Panja, B. Dietrich, A. J. Smith, A. Seddon, D. J. Adams, *ChemSystemsChem* **2022**, *4*, 202200008.
[15] a) S. Bai, C. Pappas, S. Debnath, P. W. J. M. Frederix, J. Leckie, S. Fleming, R. V. Ulijn, *ACS Nano* **2014**, *8*, 7005; b) G. G. Scott, P. J. Mcknight, T. Tuttle, R. V. Ulijn, *Adv. Mater.* **2016**, *28*, 1381.
[16] J. C. Warf, *Anal. Chem.* **1968**, *40*, 1370.
[17] a) C. A. G. N. Montalbetti, V. Falque, *Tetrahedron* **2005**, *61*, 10827; b) K. J. Padiya, S. Gavade, B. Kardile, M. Tiwari, S. Bajare, M. Mane, V. Gaware, S. Varghese, D. Harel, S. Kurhade, *Org. Lett.* **2012**, *14*, 2814.
[18] J. W. Sadownik, J. Leckie, R. V. Ulijn, *Chem. Commun.* **2011**, *47*, 728.
[19] L. L. E. Mears, E. R. Draper, A. M. Castilla, H. Su, Zhuola, B. Dietrich, M. C. Nolan, G. N. Smith, J. Doutch, S. Rogers, R. Akhtar, H. Cui, D. J. Adams, *Biomacromolecules* **2017**, *18*, 3531.
[20] a) D. Del Giudice, F. Frateloreto, C. Sappino, S. Di Stefano, *Eur. J. Org. Chem.* **2022**, *n/a*, e202200407; b) S. Panja, D. J. Adams, *Chem. - Eur. J.* **2021**, *27*, 8928.
[21] a) M. Singh, C. Berkland, M. S. Detamore, *Tissue Eng. Part B* **2008**, *14*, 341; b) F. Brandl, F. Sommer, A. Goepferich, *Biomaterials* **2007**, *28*, 134; c) R. Chen, K. Das, M. A. Cardona, L. Gabrielli, L. J. Prins, *J. Am. Chem. Soc.* **2022**, *144*, 2010.
[22] L. M. Cross, K. Shah, S. Palani, C. W. Peak, A. K. Gaharwar, *Nanomed.: Nanotech. Biol. Med.* **2018**, *14*, 2465.

